EREM 80/1
Journal of Environmental Research, Engineering and Management
Vol. 80 / No. 1 / 2024
pp. 7–20
DOI 10.5755/j01.erem.80.1.34243

Reactive Blue 19 Adsorption on Activated Carbon from Pumpkin (Cucurbita Pepo) Seed Waste: Kinetic, Isotherm and Thermodynamic Studies

Received 2023/05 | Accepted after revisions 2023/11

https://doi.org/10.5755/j01.erem.80.1.34243

Reactive Blue 19 Adsorption on Activated Carbon from Pumpkin (Cucurbita Pepo) Seed Waste: Kinetic, Isotherm and Thermodynamic Studies

Yusuf Kızıl[1], Veysel Benek[2], İbrahim Teğin[1], Yunus Önal[3], Kadir Erol[4]*, İhsan Alacabey[5]

[1] Department of Chemistry, Faculty of Arts and Science, Siirt University, Turkey

[2] Vakıfbank Secondary School, Ministry of National Education, Turkey

[3] Department of Chemistry Engineering, Faculty of Engineering, Inonu University, Turkey

[4] Department of Medical Services and Techniques, Vocational School of Health Services, Hitit University, Turkey

[5] Department of Medical Services and Techniques, Vocational School of Health Services, Mardin Artuklu University, Turkey

***Corresponding author:** kadirerol86@gmail.com

In this study, the removal of reactive blue 19 dyestuffs in aqueous systems was investigated by the adsorption method using activated carbon obtained from pumpkin seed waste. Activated carbon obtained from pumpkin seed waste functionalized with $ZnCl_2$ was used as an absorbent. Pumpkin seed hydrochar was characterized by FT-IR, SEM, TGA-DTA, BET, and XPS. In the experimental stages, the adsorption equilibrium time was determined as 45 minutes, the adsorbent dosage was 0.8 g and the optimum pH was 6.0. After this step, the adsorption parameters of Langmuir, Freundlich, Temkin, and Dubinin-Radushkevich isotherms were investigated. It has been pointed out that the adsorption process fits better with the Freundlich isotherm model, and the adhesion occurs in a multilayered manner and on a heterogeneous surface. Freundlich and Dubinin-Radushkevich isotherms support that the bonding mechanism is realized by physical interactions. When the kinetic data were evaluated, adsorption mechanism was found to be compatible with the pseudo-second-order kinetic model. The thermodynamic parameters of adsorption indicate that the system is endothermic, and the adsorption of reactive blue 19 on activated carbon is a spontaneous process.

Keywords: activated carbon, isotherm, kinetic model, pumpkin seeds, reactive blue 19.

Introduction

Water is used extensively in textile, leather, paper, food, printing, plastics, and many other dyestuffs industries (Demiral et al., 2019; Kowalkowska and Jóźwiak, 2019). As a result, large amounts of colored wastewater are produced. Depending on the dyeing technology used and the type of materials to be dyed, 10% to 50% of the dye used in the process remains in the post-production wastewater (Paz et al., 2017). When dyes are dumped directly into a landfill or a river, problems arise. Outlets turn into colored water, obstructing light penetration, reducing oxygen content, and destroying the river ecosystem (Nandiyanto et al., 2021). Therefore, it is an important environmental problem to remove the dyes from wastewater. A large number of adsorbents are used to remove dyestuffs from wastewater.

As a powerful adsorbent, activated carbon with a large surface area has been used (AntimaKatiyar and Sharma, 2014; Raji et al., 2023; Xing et al., 2023). In general, activated carbon is a microporous solid, but it also contains meso- and macropores, which are critical pores in allowing adsorbate molecules to enter the interior of carbon particles (Lashaki et al., 2023). However, the regeneration and reuse of activated carbon are costly. To overcome these drawbacks/complications, researchers must shift their focus to natural, renewable, abundant, eco-friendly, and low-cost materials as alternative adsorbents (Bozacı and Acaralı, 2023).

Theoretically, any carbonaceous material rich in elemental carbon can be used to create activated carbon. There has been a lot of research done recently on producing activated carbon from various precursors, such as orange peels (Kamińska et al., 2021), peels of bananas (Tripathy et al., 2021), walnut shells (Gao et al., 2017), coconut shells (Sujiono et al., 2022), lemon peels (Ramutshatsha-Makhwedzha et al., 2022), and cheery stones (González-Domínguez et al., 2017).

Both physical and chemical activation processes can be used to create activated carbon. The former includes first carbonizing the raw material (below 700°C), and then carefully gasifying it in a stream (air or CO_2) of an oxidizing gas at higher temperatures (> 850°C) (Zhou et al., 2018). The latter includes adding activating reagents to the raw material, such as phosphoric acid (H_3PO_4) (Zięzio et al., 2020), sulfuric acid (H_2SO_4) (Asaslan Kolur et al., 2019), zinc chloride ($ZnCl_2$) (Li et al., 2020), potassium hydroxide (KOH) (Williams et al., 2022), and potassium carbonate (K_2CO_3) (Khuong et al., 2022). Compared with the physical activation method, the chemical activation method has several advantages. It necessitates shorter activation durations and lower activation temperatures. High yields of activated carbon with a significant surface area and well-developed microporosity can be produced in only one step (Yorgun and Yıldız, 2015). The most popular adsorbent for the removal of dyestuff from wastewater is activated carbon, which is produced by utilizing $ZnCl_2$ since it has a superior high surface area and high adsorption capacity for organic compounds (Zhang et al., 2022).

This study looked at the adsorption method for removing reactive blue 19 (RB 19) dyestuff from water solutions using activated carbon made from pumpkin seed waste. As an absorbent, pumpkin seed-derived activated carbon that had been treated with $ZnCl_2$ was employed. The effects of variables including adsorption time, absorbent amount, pH variation, and temperature on adsorption were each examined in experimental experiments.

Materials and Methods

Materials

Reactive blue 19 (anthraquinone dye), zinc chloride ($ZnCl_2$, reagent grade, ≥ 98%), hydrochloric acid (HCl, ACS reagent, 37%), sodium hydroxide (NaOH, reagent grade, ≥ 98%, pellets, anhydrous), and silver nitrate ($AgNO_3$, ACS reagent, ≥ 99.0%) were supplied from Sigma-Aldrich (Taufkirchen, Germany) company. Activated carbon used as an adsorbent in adsorption studies was synthesized in the laboratory. All other chemicals are of analytical grade and the conductivity of pure water used in adsorption experiments is 18.2 MΩ.cm.

Preparation of activated carbon from pumpkin seed waste

Pumpkin seed waste was dried in an oven at 105°C for 24 h. Dried wastes were obtained to have a size of less than 4 nm by using a mortar and sieve. The wastes taken from here were mixed with $ZnCl_2$ at a ratio of 1:1 by mass, and enough water was added and impregnated.

After the samples taken from here were dried in an oven at 105°C for 24 h, they were subjected to chemical activation for 60 min at a maximum temperature of 500°C (heating rate of 10°C/min) in three zone heated furnaces in a steel reactor. When the temperature of the oven reached room temperature, the samples were taken and washed first with 0.5 N HCl and then with distilled water. Washing was continued until no chloride ions remained. Silver nitrate test was performed to determine whether chloride ions remained. After washing, activated carbon was oven-dried at 105°C for 24 h, finely ground in agar mortar, then sieved using a 35-mesh (500 µm) sieve and stored in a desiccator for analysis.

Characterization studies

The scope of the characterization in this study, X-ray photoelectron spectroscopy (XPS, PHI 5000 VersaProbe, USA) was performed to obtain chemical information about the surface of the modified activated carbon. Fourier transform infrared spectroscopy (FT-IR, Bruker Vertex 70v, USA) was used to determine the chemically functional groups in the structure of activated carbon. Besides, the weight of the sample was monitored against temperature or time with thermogravimetric differential thermal analysis (TGA/DTA, Shimadzu DTG-60H, Japan). While smanning electron Microscopy (SEM, JEOL JSM-5600LV, France) was used to observe the irregular surface of the material, the surface area of the synthesized activated carbon was determined by Brunauer-Emmett-Teller (BET, Nova 4200e Quantachrome Instruments, USA) analysis.

Adsorption experiments

In the adsorption experiments, activated carbon (modified with $ZnCl_2$) obtained from pumpkin seed waste was used as an adsorbent and the RB 19 was removed from aqueous systems. To optimize the optimum interaction conditions between adsorbent and adsorbate, different interaction times, adsorbent amounts, and pH values were studied.

First of all, the dye solution at a concentration of 1000 mg/L was prepared as a stock, and the dye solutions prepared from this stock were used in all adsorption experiments. To determine the optimum interaction time, 0.1 g of activated carbon was added to the dye solution (250 mL) prepared at a concentration of 80 mg/L and placed in a magnetic stirrer (WN-10H-120, Weightlab Instruments) with a heating function (400 rpm, 25°C). Samples were taken (2 mL) from the mixture at 15 different times in the period from the first min to the 180th min after the interaction started. These samples were centrifuged (NF 800R, Nüve) at 2000 rpm for 3 min. After centrifugation, the absorbance values of the upper liquid phase were read with a UV-VIS spectrophotometer (UV mini-1240 UV-Visible Spectrophotometer, Shimadzu) at 594 nm wavelength and the remaining dyestuff concentration in the medium was determined.

Afterward, eight samples were prepared in different glass erlenmeyer flasks from 100 mL of dye solution at a concentration of 80 mg/L. Different amounts of activated carbon (50–1200 mg) were added to each of these dye solutions separately. These mixtures were mixed at 400 rpm (at 35°C) for 45 min to determine the optimum amount of activated carbon. After the interaction was completed, 2 mL samples were taken from each flask and centrifuged at 2000 rpm for 3 min to determine the remaining amount of dye in the samples with the UV-VIS spectrophotometer (594 nm).

In the experiment in which the effect of pH value on adsorption was investigated, seven different 100 mL dye solutions (80 mg/L) were prepared from the stock solution. The equilibrium temperatures of these solutions, which were taken on the magnetic stirrer with the heating function, were fixed at 35°C and their pH values were adjusted between 2.0 and 8.0 so that each of them reached a different integer value. 0.8 g of adsorbent was added to each solution and subjected to interaction at 400 rpm for 45 min. Then, as in the previous applications, 2 mL samples were taken from each mixture and centrifuged. The remaining dye amounts were analyzed spectroscopically and the optimum pH value was determined for the adsorption interaction.

The amount of dye adsorbed per unit activated carbon (mg/g) and as a percentage (%) was obtained as follows.

$$q_e = \frac{(C_0 - C_e)V}{m} \quad (1)$$

$$\text{Adsorption } (\%) = \frac{C_0 - C_e}{C_0} \text{ x100} \quad (2)$$

Where: C_o– the starting concentration of dye in solution (mg/L); C_e – final dye concentration in solution (mg/L); V – the volume of the solution (L); m – the weight of activated carbon (g).

Isotherm and kinetic studies

Dye removal was investigated under optimum conditions for adsorption isotherm-kinetic models and thermodynamic parameters. In parallel with this idea, the adsorption parameters of Langmuir, Freundlich, Temkin, and Dubinin-Radushkevich (D-R) isotherms were calculated. The Langmuir isotherm assumes that there are adsorbent points on the adsorbent surface. It explains that the resulting layer can be a single molecule layer, assuming that each adsorbing spot adsorbs a single molecule. According to the Freundlich approach, the adsorption areas on the adsorbent surface are seen as heterogeneous. In other words, the adsorption areas consist of different adsorption areas. The Temkin model clearly reveals the adsorbate-adsorbent interaction. It predicts that the heat of adsorption (temperature function) of all molecules in the layer, regardless of very low and very high concentration data, will decrease linearly rather than logarithmically as the surface wraps. Besides, the average adsorption energy (E) from the D-R isotherm provides information on the chemical and physical properties of adsorption. The D-R isotherm takes a more inclusive approach than the Langmuir isotherm, as it does not rely on a homogeneous surface and a constant adsorption potential. All isotherms and their equations examined within the scope of the study are given in *Table 1*.

Table 1. *Isotherm models and equations*

Isotherm Model	Equation
Langmuir	$\frac{C_e}{q_e} = \frac{1}{q_m} * C_e + \frac{1}{K_L q_m}$ (7) C_e – adsorbate concentration at equilibrium (mg/L); q_e – amount of adsorbate adsorbed per gram adsorbent at equilibrium (mg/g); q_m – maximum single-layer adsorption capacity (mg/g); K_L –Langmuir isotherm constant (L/mg).
Freundlich	$\log q_e = \log K_F + \frac{1}{n} \log C_e$ (8) C_e – adsorbate concentration at equilibrium (mg/L); q_e – amount of adsorbate adsorbed per gram adsorbent at equilibrium (mg/g); K_F – Freundlich constant, adsorption capacity (L/mg); N – adsorption intensity (density).
Temkin	$q_e = B \ln K_T + B \ln C_e$ (9) $B = \frac{RT}{b}$ (10) C_e – equilibrium concentration (mg/L); K_T – Coupling constant at equilibrium (L/g); B – Temkin isotherm constant (L/mg); R – universal gas constant (8.314 J/mol K); T – temperature (K); B – constant depending on the heat of adsorption (J/mol).
Dubinin-Radushkevich	$\ln q_e = \ln q_m - k_{D-R} \varepsilon^2$ (11) $\varepsilon = RT \ln(1 + \frac{1}{C_e})$ (12) $E = (2k_{D-R})^{\frac{-1}{2}}$ (13) E – Polanyi potential; q_e – the amount of adsorbate retained per unit weight of the adsorbent (mg/g); q_m – maximum adsorption capacity (mg/g); C_e – equilibrium concentration (mg/L); R – universal gas constant (8.314 J/mol K); T – temperature (K); k_{D-R} – D-R isotherm constant; E – average adsorption energy.

In experimental applications, adsorption was worked at three different temperatures as 25°C, 35°C, and 45°C, respectively. Five dye solutions (100 mL) of 10 mg/L, 20 mg/L, 40 mg/L, 60 mg/L, and 80 mg/L were obtained by dilution from the stock. These solutions were placed in the magnetic stirrer with the heating function and the stirrer speed was adjusted to 400 rpm. After the solution temperature reached equilibrium, the pH values of the solutions were adjusted to 6.0, and 0.8 g of adsorbent was added to each of the solutions. After 45 min of interaction, 2 mL of liquid was taken from the medium and centrifuged at 2000 rpm for 3 min. In the last step, the samples were analyzed in the UV-VIS spectrophotometer at a wavelength of 594 nm. Thus, the remaining dyestuff concentration in the sample was calculated.

In addition, 50 mL of 80 mg/L dye solution was used for the kinetic study. The temperature was set at 25°C and the solution was left on the magnetic stirrer at 400 rpm. The temperature was allowed to reach the equilibrium temperature and after the pH of the solution was adjusted to 6.0, activated carbon (0.8 g) was added to the solution. After 1, 3, 5, 7, 9, 15, 20, 30, 40, 60, and 75 min after the interaction started, a 2 mL sample was taken from the mixture and centrifuged (2000 rpm, 3 min). The amount of dye remaining in the samples was again

determined spectrophotometrically. This study was repeated for the temperature values at 35°C and 45°C. For the kinetic investigation of the adsorption interaction, pseudo-first-order, pseudo-second-order, and intraparticle diffusion model were studied. The equations of these models are presented in *Table 2*. In addition, adsorption parameters (ΔH^o, ΔS^o, and ΔG^o) were calculated to determine the adsorption thermodynamics.

$$\Delta G^o = \Delta H^o - T\Delta S^o \quad (3)$$

Where: ΔG^o – standard Gibbs free energy change, kJ/mol; ΔH^o – standard enthalpy change, kJ/mol; ΔS^o – standard entropy change, kJ/mol K; T – absolute temperature, K; R – ideal gas constant, 8.314 kJ/mol K.

Table 2. *Kinetic models and equations*

Kinetic Models	Equations
Pseudo-first-order	$\log(q_e - q_t) = \log(q_e) - \frac{k_1}{2.303} * t$ (14) q_e – the amount of adsorbate adsorbed per gram of adsorbent at equilibrium (mg/g); q_t – the amount of adsorbate adsorbed per gram of adsorbent at any one time (mg/g); k_1 – Rate constant (1/min); t – Contact time (min).
Pseudo-second-order	$\frac{t}{q_t} = \frac{1}{k_2 * q_e^2} + \frac{t}{q_e}$ (15) q_e – The amount of adsorbate adsorbed per gram of adsorbent at equilibrium (mg/g); q_t – The amount of adsorbate adsorbed per gram of adsorbent at any one time (mg/g); k_2 – Rate constant (1/min); t – Contact time (min).
Intraparticle diffusion	$q_t = k_{id} * t^{\frac{1}{2}} + C$ (16) q_t – The amount of substance adsorbed at the end of t time (mg/g); k_{id} – Intraparticle diffusion rate constant (mg/g $min^{1/2}$); t – Adsorption time (min); C – Constant related to the boundary layer thickness formed between adsorbent and adsorbate (mg/g).

To find the Gibbs free energy of the adsorption process at a certain temperature;

$$K_c = \frac{C_a}{C_e} \quad (4)$$

Where: K_c – equilibrium constant of adsorption; C_a – the amount of substance retained in the unit mass of the adsorbent (mg/g); C_e – adsorbate concentration remaining in solution after adsorption (mg/L).

Using the above-mentioned equation, K_c is placed in the following equation to obtain the standard Gibbs free energy for adsorption:

$$\Delta G^o = -R\,T\,\ln K_c \quad (5)$$

Using the equation below, the slope of the line created by plotting the $\ln K_c$ value according to the 1/T value gives ΔH° and the intersection point gives ΔS°.

$$\ln K_c = \frac{\Delta S^o}{R} - \frac{\Delta H^o}{RT} \quad (6)$$

Results and Discussion

Characterizations

The XPS analysis spectrum of activated carbon obtained from pumpkin seed waste functionalized with $ZnCl_2$ is given in *Fig. 1*. It can be seen in the XPS spectrum of the sample that it contains mostly carbon elements in the structure with a binding energy of about 285 eV. In the spectrum, there are also peaks belonging to Zn and Cl atoms in very small proportions. The probable cause of these peaks may be related to residues left after treatment of the sample with $ZnCl_2$.

The FT-IR spectrum of activated carbon modified using $ZnCl_2$ before and after RB 19 adsorption is shown in *Fig. 2*. The broad band observed in the range of 3500–3000 cm^{-1} in the spectrum of activated carbon before the adsorption process belongs to the stretching vibration peak of the (O–H) group caused by phenol, alcohol, and absorbed water (*Fig. 2a*). The absorption peak observed at 2923 cm^{-1} belongs to the asymmetric vibration of the (–C–H) group. The absorption peak observed around 2360 cm^{-1} indicates acetylene vibration. The peak at 1580 cm^{-1} is due to bands of C=C

stretching vibrations of highly conjugated carbonyls in the aromatic ring. It is thought that the peaks are seen at 1190 cm^{-1} and 1040 cm^{-1} correspond to the stretching vibration of C–O in the structure of activated carbon. The obtained peaks show that the synthesis of activated carbon from pumpkin seed waste is successful and is compatible with the literature (Nurfatimah, 2018; Al-Layla and Fadhil, 2022).

The FT-IR spectrum of activated carbon after dye adsorption is shown in *Fig. 2b*. The intense peak between 3350–3650 cm^{-1} is due to the stretching vibration of the hydroxyl group. C–H stretching peak was observed at 2950 cm^{-1}. The weak band at 1600 cm^{-1} corresponds to the aromatic stretch of the C=C group. The stretching of C=C in aromatic compounds causes an increase in intermolecular charge transfer between donor and acceptor electrons. The peak at 1480 cm^{-1} is due to the bending of the C–H group. It is estimated that the vibration at 1090 cm^{-1} is due to the S=O stretching in the sulfonate groups in the dye. The obtained peaks confirm the successful adsorption of RB 19 with activated carbon obtained from pumpkin seed waste (Nurfatimah, 2018; Al-Layla and Fadhil, 2022; Jeyaram et al., 2021).

As can be seen from the TG/DTA curves of the synthesized activated carbon, there are two-stage mass losses with temperature (*Fig. 3*). A weight loss of 8.5% was observed in the first region at approximately 100°C and a weight loss of 64.2% in the second region at 463°C and later. It can be noticed from the TG/DTA curves that approximately 30% of the sample remains. In order to improve the elimination of volatiles like H_2 and O_2 from the carbon matrix, $ZnCl_2$ works as a dehydrating agent. Since it is extremely soluble in

Fig. 1. *XPS analysis spectrum of activated carbon from pumpkin seed waste treated with $ZnCl_2$*

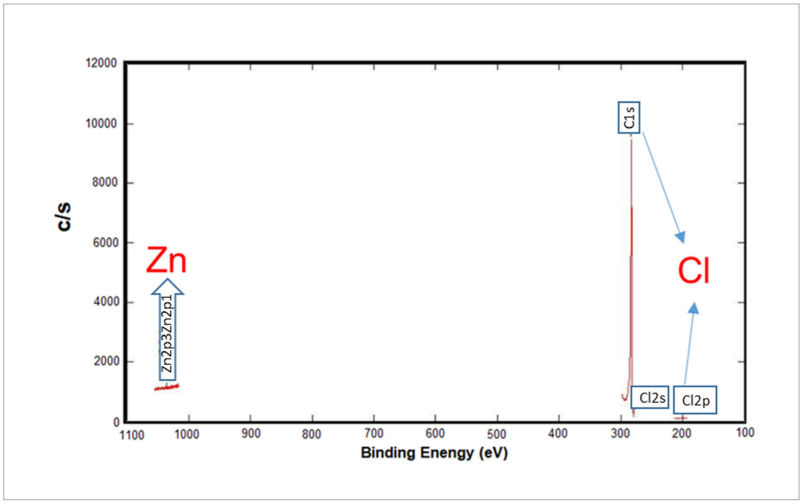

Fig. 2. *FT-IR spectrum of activated carbon before (a) and after (b) dye adsorption*

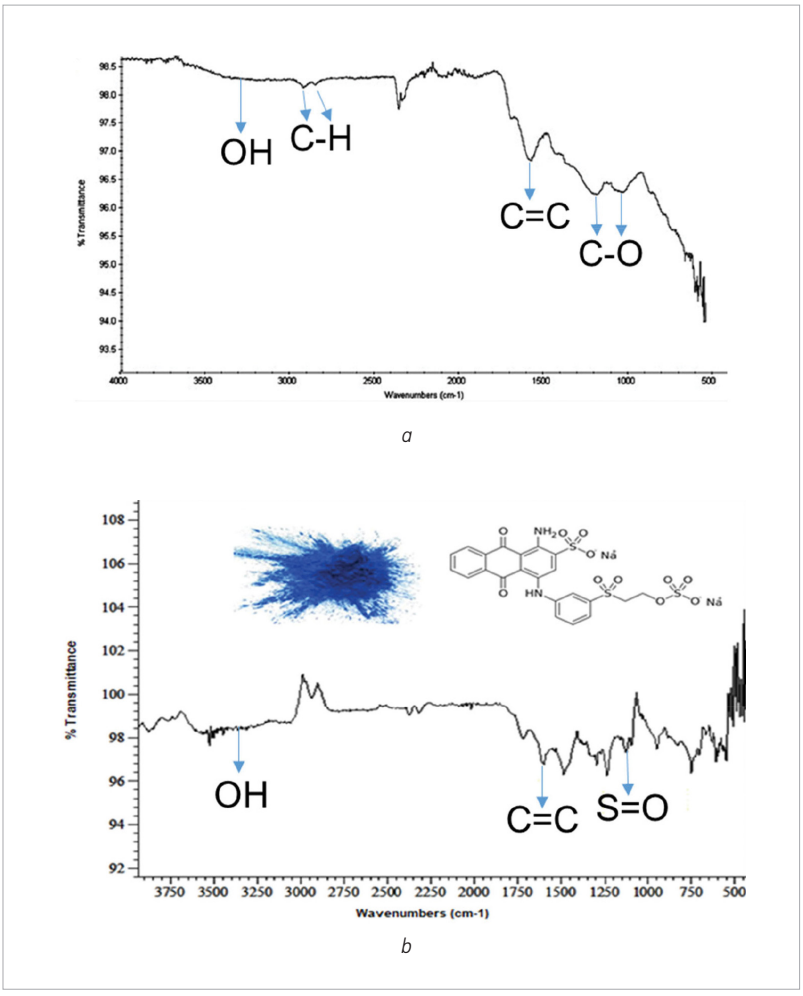

Fig. 3. *DTA/TGA analysis of activated carbon from pumpkin seed waste functionalized with $ZnCl_2$*

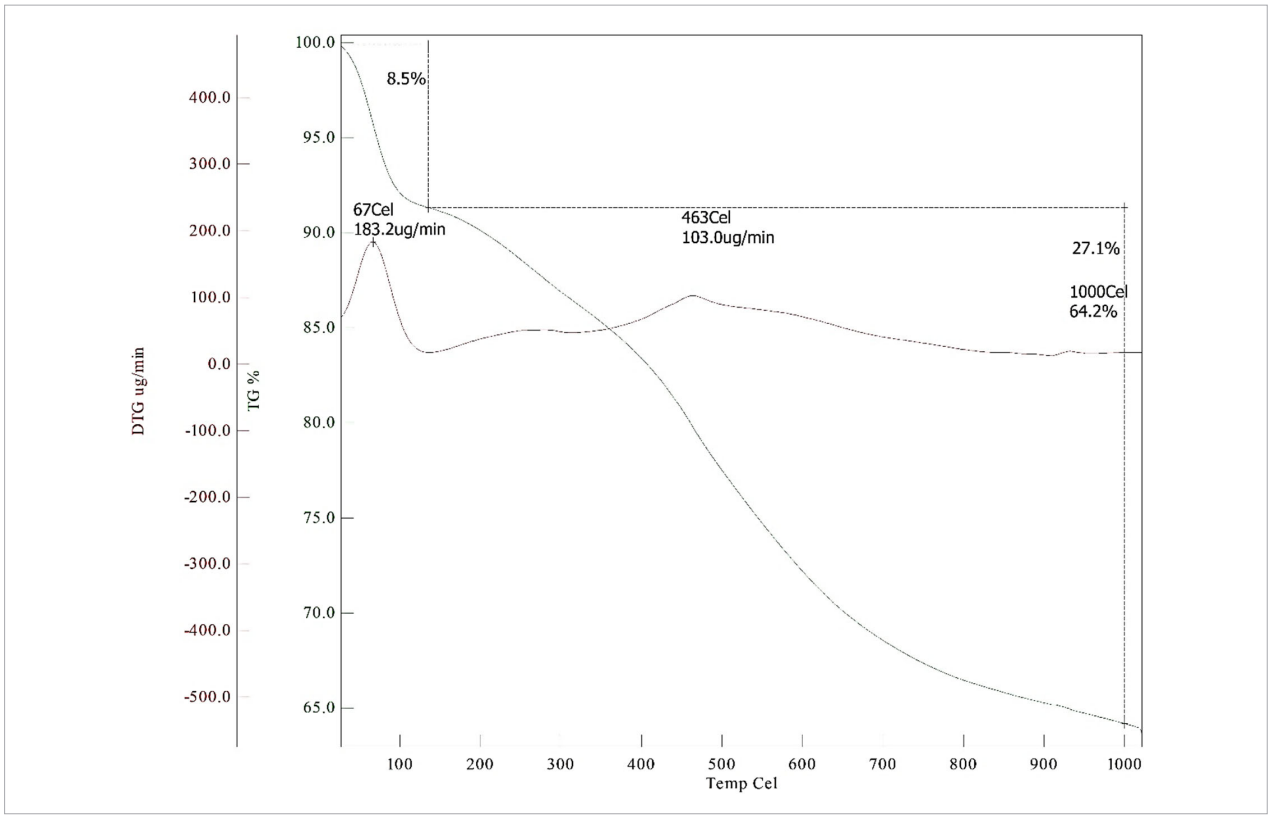

water, the elimination of water and volatile compounds is accelerated. Because $ZnCl_2$ breaks down aromatic and aliphatic chains, it can hasten the evaporation of volatiles in high concentrations (Zubir and Zaini, 2020). Weight loss at low temperatures is related to the loss of physically adsorbed water and volatile components. In the studies, material losses occurring in the temperature range of 280–400°C and 140–900°C were attributed to the degradation of cellulose and lignin (Zhu et al., 2016).

SEM images of activated carbon obtained from pumpkin seed waste before and after adsorption are given in *Fig. 4*, respectively. When the figures are examined, physical differences can be seen. While there was a more bulky image before adsorption, a more fragmented image was noticed after adsorption. Besides, according to the results of BET analysis, the surface area of activated carbon modified with $ZnCl_2$ obtained from pumpkin seed waste was determined as 69.7 m^2/g. This value makes it logical that RB 19 is effectively adsorbed by activated carbon from pumpkin seed waste.

Fig. 4. *SEM images of activated carbon before (a) and after (b) adsorption*

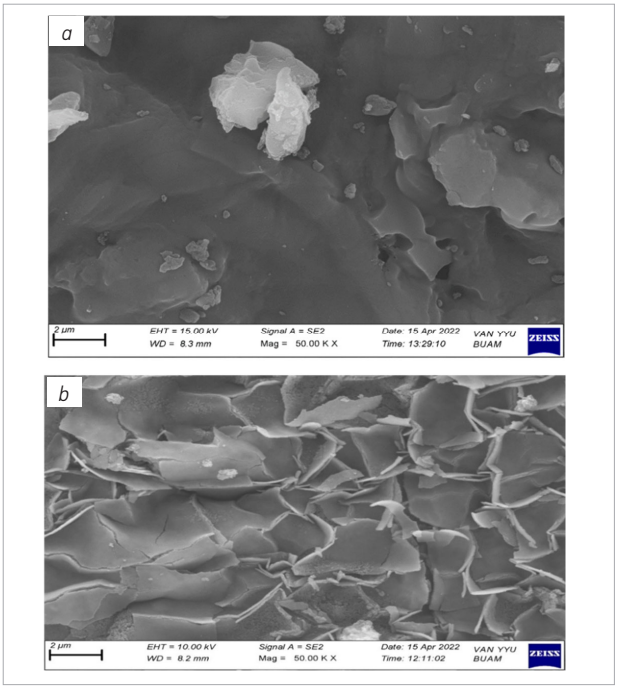

Adsorption experiments

The graph obtained as a result of the study to determine the optimum interaction time is given in *Fig. 5.* When the graph was examined, it was observed that the amount of RB 19 adsorbed by activated carbon increased with the interaction time in the first 45 min. After the 45th min, there was no significant increase. This is because, after this minute, the active sites of the activated carbon that adsorb dye are completely saturated with the adsorbate molecules.

Experimental studies were carried out with different amounts of activated carbon and the resulting graph is presented in *Fig. 6.* First of all, an increase in adsorption was determined in direct proportion to the increase in the amount of adsorbent. It was observed that in the amount of 0.8 g activated carbon, the graph reached the maximum point, and in the amounts of 1.0 and 1.2 g adsorbent, there were slight decreases in the percentage of adsorption compared with the study using 0.8 g activated carbon. Probably the reason for these decreases may be that in the presence of more than 0.8 g of activated carbon, the adsorbent molecules interact not only with the dye but also with each other and prevent dye adsorption to some extent (Gorzin and Abadi, 2018).

In the adsorption study performed at different pH values, it was noticed that the adsorption amount was lower at low pH points, and the adsorption percentage increased in the slightly acidic-neutral pH region (*Fig. 7*). The optimum value was determined as 6.0, especially for the adsorption interaction reaching the highest amount at this point. This pH value is estimated as the grade where the loaded groups in the adsorbent and adsorbate interact most comfortably.

When literature is searched on the removal of RB 19 from aqueous media, a study in which rice straw fly ash is used as an addsorbant draws attention (El-Bindary et al., 2016). In this study, a removal percentage of over 85% was reported in highly acidic conditions at a 60-min interaction time. In another study, RB 19 was removed from aqueous solutions over pomegranate residual-based activated carbon and a removal rate of 98.7% was achieved (Radaei et al., 2014). Besides, successful results were obtained in removing RB 19 from the aqueous environment by using pomegranate seed powder as an adsorbent. In addition, by using pomegranate seed powder as an adsorbent, successful results were obtained in the removal of RB 19 from the aqueous environment under optimum adsorption conditions, and removal efficiency from 87% to 100% was achieved depending on the dye concentration (Dehvari et al., 2016). In a recent study in which hydrogel was used as an adsorbent, 80% of RB 19 was removed from the aqueous medium with a kind of Guar gum-based polymer (Matho and Mishra, 2022). As it can be seen from these results,

Fig. 5. *Adsorption study with different interaction times (V – 250 mL, C_o – 80 mg/L, m – 0.1 g, T – 298 K)*

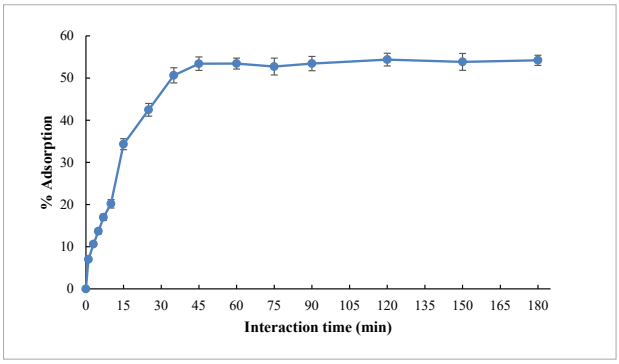

Fig. 6. *The effect of different adsorbent amounts on adsorption (V – 100 mL, C_o – 80 mg/L, T – 308 K, t – 45 min)*

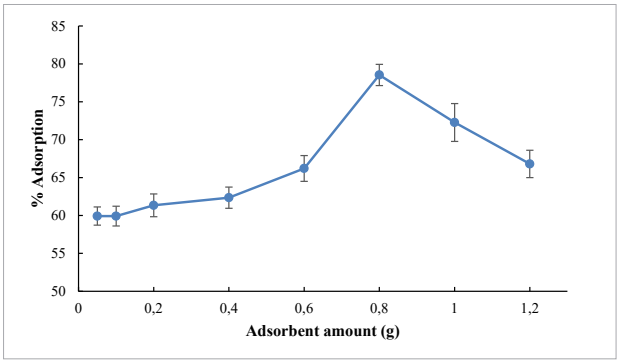

Fig. 7. *The effect of changing pH values on the adsorption percentage (V – 100 mL, C_o – 80 mg/L, m – 0.8 g, T – 308 K, t – 45 min)*

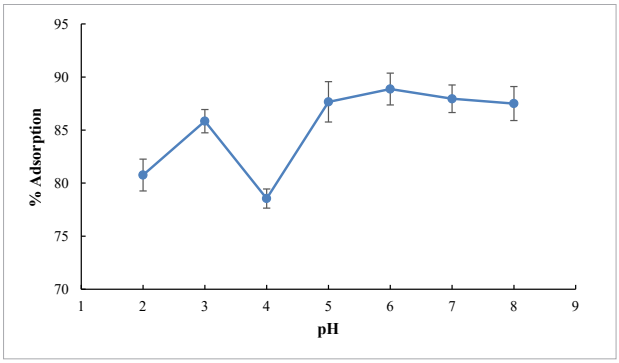

the approximately 89% removal rate of RB 19 we obtained in our study is comparable to the literature.

Isotherm studies

To examine the isotherm of the adsorption interaction, experiments were performed at three different temperatures and five different adsorbate concentrations, and the results are given in *Table 3*. Based on these data and using the equations in *Table 1*, all parameters of Langmuir, Freundlich, Temkin, and D-R isotherm models were calculated and presented in *Table 4*. (All isotherm graphs are provided in the Supplementary Information-SI)

In the graphs drawn to calculate the Langmuir isotherm constants, the correlation factor of RB 19 adsorption on activated carbon at 298 K, 308 K, and 318 K was found to be R^2 = 0.8656, R^2 = 0.7406 and R^2 = 0.6963, respectively (SI-*Fig. 1*). The curves were drawn to calculate the Freundlich isotherm constants under the same conditions, and the correlation factors were calculated at 298 K (R^2 = 0.9902), 308 K (R^2 = 0.9631), and 318 K (R^2 = 0.9481) (SI-*Fig. 2*). In line with these results, since the correlation factor (R^2) values obtained for the Freundlich isotherm are higher than the Langmuir isotherm model, the adsorption of RB 19 on activated carbon is more compatible with the Freundlich isotherm model. Besides, Freundlich constant (adsorption capacity, K_F) values vary between 1.77–2.46 mg/g depending on the working temperature range. It is concluded that the interaction in the system is endothermic due to the K_F values increasing with the increase in temperature. For the value of n, which is a constant that determines the type of process, it turns out that the adsorption is linear if n = 1, the process is chemical adsorption if n < 1, and the process is physical adsorption if n > 1. As it can be seen in *Table 4*, the 1/n value is 0.5898, 0.5833, and 0.5562 at temperatures of 298 K, 308 K, and 318 K, respectively. Thus, the n values in our experimental study were calculated as 1.6956, 1.7143, and 1.7979 for all investigated temperatures. The n > 1 phenomenon is the most common and may be caused by any factor that causes the distribution of surface areas or the decrease in adsorbent-adsorbate interaction with increasing surface density. The n values calculated for the three different temperature values studied show that the adsorption of RB 19 on the activated carbon occurs by physical interaction (Alacabey, 2022a; Alacabey, 2022b).

Table 3. *Adsorption data for RB 19 adsorption on activated carbon at different temperatures*

Temperature (K)	C_o (mg/L)	C_e (mg/L)	q_e (mg/g)	C_e/q_e (g/L)	% Adsorption
298	10.00	0.47	1.19	0.39	95.31
	20.00	1.72	2.29	0.75	91.43
	40.00	4.92	4.39	1.12	87.70
	60.00	9.64	6.30	1.53	83.94
	80.00	11.87	8.52	1.39	85.16
308	10.00	0.31	1.21	0.26	96.88
	20.00	1.66	2.29	0.73	91.68
	40.00	3.91	4.51	0.87	90.22
	60.00	7.42	6.57	1.13	87.64
	80.00	8.67	8.92	0.97	89.16
318	10.00	0.22	1.22	0.18	97.79
	20.00	1.51	2.31	0.65	92.47
	40.00	3.30	4.59	0.72	91.75
	60.00	6.02	6.75	0.89	89.97
	80.00	7.55	9.06	0.83	90.56

Table 4. *All adsorption parameters of adsorption interaction*

T (K)	Langmuir			Freundlich			
	K_L (L/mg)	q_m (mg/g)	R^2	n	1/n	K_F (mg/g)	R^2
298	0.1652	11.3439	0.8656	1.6956	0.5898	1.7701	0.9902
308	0.1801	12.5841	0.7406	1.7143	0.5833	2.1194	0.9631
318	0.2086	12.9893	0.6963	1.7979	0.5562	2.4603	0.9481
T (K)	Temkin			Dubinin-Radushkevich			
	b (kJ/mol)	K_T (L/mg)	R^2	q_m (mg/g)	E (kJ/mol)	R^2	
298	1.1920	2.6082	0.8807	5.3427	1.5830	0.7469	
308	1.2296	3.6053	0.8184	5.3455	2.0854	0.6932	
318	1.3192	4.9837	0.7974	5.3778	2.5752	0.6770	

The Temkin isotherm model shows a linear decrease in the heat of adsorption for all molecules. The b data (1.192–1.319 kJ/mol) obtained as a result of this experimental study show the weak ionic interaction between the adsorbate and the adsorbent. This is proof of the homogeneity in the binding energy of the molecules to the adsorbent, and it can be said that the adsorption interaction is physical. At the same time, the Freundlich and Langmuir isotherms are insufficient to explain the physical and chemical properties of adsorption. The D-R isotherm is more general than the Langmuir isotherm as it does not assume a homogeneous surface or a constant adsorption potential. The average adsorption energy E (kJ/mol) in the D-R isotherm expresses the adsorption energy that gives information about the chemical or physical properties of adsorption. Since the E value is < 8 kJ/mol, it is concluded that adsorption is physical adsorption (Alacabey, 2022b).

Kinetic calculations

To determine the kinetic mechanism of the adsorption interaction, it was studied at three different temperatures and eleven different interaction times, and the data obtained are shared in *Table 5*. Graphs were obtained for the pseudo-first-order kinetic model, pseudo-second-order kinetic model, and intraparticle diffusion model calculated with the equations in *Table 2* (SI-*Fig. 5–7*). The data obtained by using these graphs are given in *Table 6*. When all these data are evaluated, the correlation factor (R^2) values for the kinetic models are higher for the pseudo-second-order kinetic model, and in addition, the $q_{e\ (calc)}$ values in this kinetic model are in better agreement with the experimentally found $q_{e\ (exp)}$ values. Therefore, the adsorption system fits this kinetic model.

Thermodynamic parameters

The thermodynamic parameters obtained with the help of the graphs drawn by using the equations in Eq. 4, Eq. 5, and Eq. 6 are given in *Table 7*. When the table is examined, it is seen that the ΔH° value is less than 40 kJ/mol. This result indicates that the adsorption is physical (Kul et al., 2010). In addition, due to the positive ΔH° value, the adsorption of RB 19 dyestuff on activated carbon was found to be endothermic (Depci et al., 2011). Besides, the ΔS° value was calculated as 0.0749 kJ/mol. Positive values of entropy may be due to some structural changes in the adsorbate and adsorbent during the adsorption process in an aqueous solution. Moreover, the positive value of ΔS° indicates increased randomness at the solid-liquid interface during the adsorption of RB 19 onto activated carbon. ΔG° values for the adsorption of RB 19 on activated carbon are negative and these values indicate that the adsorption is spontaneous. These values decrease with increasing temperature and better adsorption is obtained at higher temperatures (Caliskan et al., 2011).

Table 5. *Kinetic data of the adsorption of RB 19 dye on activated carbon*

Temperature (K)	t (min)	C_o (mg/L)	C_e (mg/L)	q_t (mg/g)	q_e (mg/g)	t/q_t ((min g)/mg))
298	1	80	73.980	0.376	4.578	2.658
	3	80	49.810	1.887	4.578	1.590
	5	80	44.380	2.226	4.578	2.246
	7	80	41.740	2.391	4.578	2.927
	10	80	37.380	2.664	4.578	3.754
	15	80	29.920	3.130	4.578	4.792
	25	80	22.530	3.592	4.578	6.960
	35	80	15.080	4.058	4.578	8.626
	45	80	7.700	4.519	4.578	9.959
	60	80	7.270	4.546	4.578	13.200
	75	80	6.750	4.578	4.578	16.382
308	1	80	72.240	0.485	4.829	2.062
	3	80	49.700	1.894	4.829	1.584
	5	80	40.200	2.488	4.829	2.010
	7	80	37.050	2.684	4.829	2.608
	10	80	34.100	2.869	4.829	3.486
	15	80	26.070	3.371	4.829	4.450
	25	80	18.310	3.856	4.829	6.484
	35	80	12.830	4.198	4.829	8.337
	45	80	6.980	4.564	4.829	9.860
	60	80	2.660	4.834	4.829	12.413
	75	80	2.740	4.829	4.829	15.532
318	1	80	72.110	0.493	4.884	2.028
	3	80	49.590	1.901	4.884	1.578
	5	80	38.090	2.619	4.884	1.909
	7	80	33.940	2.879	4.884	2.432
	10	80	27.640	3.273	4.884	3.056
	15	80	21.380	3.664	4.884	4.094
	25	80	10.690	4.332	4.884	5.771
	35	80	7.390	4.538	4.884	7.712
	45	80	4.020	4.749	4.884	9.476
	60	80	1.850	4.884	4.884	12.284
	75	80	1.860	4.884	4.884	15.357

Table 6. *Kinetic parameters of adsorption mechanism*

		298 K	308 K	318 K
Pseudo-first-order kinetic model	k_1	0.0802	0.0548	0.0723
	$q_{e\ (calc)}$	4.3418	3.5454	3.6542
	$q_{e\ (exp)}$	4.5781	4.8288	4.8838
	R^2	0.9450	0.9710	0.9860
Pseudo-second-order kinetic model	k_2	0.0637	0.0516	0.0423
	$q_{e\ (cal)}$	5.1635	5.3387	5.3810
	$q_{e\ (exp)}$	4.5781	4.8288	4.8838
	R^2	0.9920	0.9960	0.9970
Intraparticle diffusion model	k_{id}	0.4928	0.5020	0.5059
	R^2	0.8950	0.8920	0.8390

Table 7. *Thermodynamic parameters of adsorption interaction*

T (K)	$\ln K_c^\circ$	ΔH° (kJ/mol)	ΔS° (kJ/mol)	ΔG° (kj/mol)
298	0.6370	20.7502	0.0749	–1.5782
308	0.9163			–2.346
318	1.1636			–3.076

Conclusions

In this study, reactive blue 19 dye removal from the aqueous solution with activated carbon obtained from pumpkin seed waste was studied. For this purpose, experimental studies were carried out with different initial concentrations at 25°C, 35°C, and 45°C temperatures and optimum pH, respectively, and the results of the experiments were applied to Langmuir, Freundlich, Temkin, and Dubinin-Radushkevich (D-R) isotherms. At the same time, the thermodynamic parameters of the adsorption interaction (ΔG°, ΔH°, and ΔS°) were found and the results were interpreted. When we looked at the correlation coefficient (R^2) values, which helped us in comparing the isotherm suitability of the adsorption study, it was seen that these values ranged between 0.94 and 0.99 in the Freundlich isotherm model and were higher than all other models. This is explained by the assumption that the adsorption process takes place on a heterogeneous surface and the adhesion is multilayered. It has been determined that the Freundlich constant (K_F) takes values between 1.7701 and 2.4603 mg/g and these values increase with the increase in temperature, so our system is endothermic. Due to the fact that the adsorption energy (E) calculated using the D-R isotherm model is less than 8 kJ/mol, it was concluded that the binding mechanism occurs through physical interactions. As a result of kinetic studies, it was determined that the adsorption mechanism complies with the pseudo-second-order adsorption kinetics. ΔG°, ΔH°, and ΔS° parameters were found as a result of thermodynamic calculations. A positive ΔH° indicated that there was an endothermic adsorption. The positive value of entropy (ΔS°) indicates that the disorder of the molecules increases during adsorption. In this study, it was determined that the values of ΔG°, decrease with increasing temperature. The negative values of ΔG° indicate that the adsorption takes place spontaneously. When all our data are evaluated, it shows that activated carbon produced from pumpkin seed waste hydrochar can be used as a suitable adsorbent for RB 19 dye.

Acknowledgements

All authors contributed to the study conception and design. Material preparation, data collection and analysis were performed by Yunus Kızıl, Veysel Benek, İbrahim Teğin, Yunus Önal, Kadir Erol and İhsan Alacabey. The first draft of the manuscript was written by Kadir Erol and İhsan Alacabey and all authors commented on previous versions of the manuscript. All authors read and approved the final manuscript.

References

Alacabey İ. (2022a) Adsorptive removal of cationic dye from aqueous solutions using Bardakçı clay. International Journal of Agriculture Environment and Food Sciences 6: 80-90. https://doi.org/10.31015/jaefs.2022.1.12

Alacabey İ. (2022b) Antibiotic removal from the aquatic environment with activated carbon produced from pumpkin seeds. Molecules 27: 1380. https://doi.org/10.3390/molecules27041380

Al-Layla A.M. and Fadhil A.B. (2022) Removal of Calcium over Apricot Shell Derived Activated Carbon: Kinetic and thermodynamic study. Chemical Methodologies 6: 10-23.

AntimaKatiyar A. and Sharma U. (2014) Utilization of waste material: pumpkin seed waste, as an efficient adsorbent for the removal of metal cutting fluids from aqueous medium/industrial waste water. International Journal of Engineering and Technology Research 2: 352-358.

Asaslan Kolur N., Sharifian S. and Kaghazchi T. (2019) Investigation of sulfuric acid-treated activated carbon properties. Turkish Journal of Chemistry 43: 663-675. https://doi.org/10.3906/kim-1810-63

Bozacı G. and Acaralı N. (2023) Chemical production of activated carbon from green coffee with adsorption isotherm support by Taguchi model. Journal of the Indian Chemical Society 100: 100864. https://doi.org/10.1016/j.jics.2022.100864

Caliskan N., Kul A.R., Alkan S., Gokirmak Sogut E. and Alacabey İ. (2011) Adsorption of Zinc (II) on diatomite and manganese-oxide-modified diatomite: A kinetic and equilibrium study. Journal of Hazardous Materials 193: 27-36. https://doi.org/10.1016/j.jhazmat.2011.06.058

Dehvari M., Ghaneian M.T., Ebrahimi A., Jamshidi B. and Mootab M. (2016) Removal of reactive blue 19 dyes from textile wastewater by pomegranate seed powder: isotherm and kinetic studies. International Journal of Environmental Health Engineering 5: 5. https://doi.org/10.4103/2277-9183.179204

Demiral İ., Bektaş T. and Şamdan C. (2019) Utilization of activated carbon prepared from pumpkin seed shell for the removal of dyestuff from aqueous solutions and wastewater by microwave radiation. International Journal of Scientific and Technology Research 5: 68-77.

Depci T., Alkan S., Kul A., Önal Y., Alacabey İ. and Dişli E. (2011) Characteristic properties of adsorbed catalase onto activated carbon based adiyaman lignite. Fresenius Environmental Bulletin 20: 2371-2378.

El-Bindary A., Abd El-Kawi M., Hafez A., Rashed I. and Aboelnaga E. (2016) Removal of reactive blue 19 from aqueous solution using rice straw fly ash. Journal of Materials and Environmental Science 7: 1023-1036.

Gao X., Wu L., Wan W., Xu Q. and Li Z. (2017) Preparation of activated carbons from walnut shell by fast activation with H_3PO_4: influence of fluidization of particles. International Journal of Chemical Reactor Engineering 16: 20170074. https://doi.org/10.1515/ijcre-2017-0074

González-Domínguez J.M., Alexandre-Franco M., Fernández-González C., Ansón-Casaos A. and Gómez-Serrano V. (2017) Activated carbon from cherry stones by chemical activation: Influence of the impregnation method on porous structure. Journal of Wood Chemistry and Technology 37: 148-162. https://doi.org/10.1080/02773813.2016.1253101

Gorzin F. and Abadi M.M.B.R. (2018) Adsorption of Cr(VI) from aqueous solution by adsorbent prepared from paper mill sludge: Kinetics and thermodynamics studies. Adsorption Science and Technology 36(1-2):149-169. https://doi.org/10.1177/0263617416686976

Jeyaram S., Naseer J. and Punitha S. (2021) Effect of solvent on third-order nonlinear optical behavior of reactive blue 19 dye. Journal of Fluorescence 31: 1895-1906. https://doi.org/10.1007/s10895-021-02808-y

Kamińska A., Miądlicki P., Kiełbasa K., Kujbida M., Sreńscek-Nazzal J., Wróbel R.J. and Wróblewska A. (2021) Activated Carbons Obtained from Orange Peels, Coffee Grounds, and Sunflower Husks-Comparison of Physicochemical Properties and Activity in the Alpha-Pinene Isomerization Process. Materials 14: 7448.https://doi.org/10.3390/ma14237448

Khuong D.A., Trinh K.T., Nakaoka Y., Tsubota T., Tashima D., Nguyen H.N. and Tanaka D. (2022) The investigation of activated carbon by K_2CO_3 activation: Micropores-and macropores-dominated structure. Chemosphere 299: 134365. https://doi.org/10.1016/j.chemosphere.2022.134365

Kowalkowska A. and Jóźwiak T. (2019) Utilization of pumpkin (Cucurbita pepo) seed husks as a low-cost sorbent for removing anionic and cationic dyes from aqueous solutions. Cellulose 171: 397-407. https://doi.org/10.5004/dwt.2019.24761

Kul A.R., Alacabey İ. and Çalışkan Kılıç N. (2010) Removal of Cobalt Ions from Aqueous Solution by Diatomite. Hacettepe Journal of Biology and Chemistry 38: 85-93.

Lashaki M.J., Kamravaei S., Hashisho Z., Phillips J.H., Crompton D., Anderson J.E. and Nichols M. (2023) Adsorption and Desorption of a Mixture of Volatile Organic Compounds: Impact of Activated Carbon Porosity. Separation and Purification Technology 314: 123530. https://doi.org/10.1016/j.seppur.2023.123530

Li B., Hu J., Xiong H. and Xiao Y. (2020) Application and properties of microporous carbons activated by ZnCl2: adsorption behavior and activation mechanism. ACS Omega 5: 9398-9407. https://doi.org/10.1021/acsomega.0c00461

Mahto A. and Mishra S. (2022) The removal of textile industrial Dye-RB-19 using Guar gum-based adsorbent with thermodynamic and kinetic evaluation parameters. Polymer Bulletin 79: 3353-3378. https://doi.org/10.1007/s00289-021-03663-4

Nandiyanto A.B.D., Hofifah S.N., Inayah H.T., Putri S.R., Apriliani S.S., Anggraeni S., Usdiyana D.and Rahmat A. (2021) Adsorption isotherm of carbon microparticles prepared from pumpkin (Cucurbita maxima) seeds for dye removal. Iraqi Journal of Science 62: 1404-1414. https://doi.org/10.24996/ijs.2021.62.5.2

Nurfatimah R. (2018) Preparation of polyethylene glycol diglycidyl ether (PEDGE) crosslinked chitosan/activated carbon composite film for Cd^{2+} removal. Carbohydrate Polymers 199: 499-505. https://doi.org/10.1016/j.carbpol.2018.07.051

Paz A., Carballo J., Pérez M.J. and Domínguez J.M. (2017) Biological treatment of model dyes and textile wastewaters. Chemosphere 181: 168-177. https://doi.org/10.1016/j.chemosphere.2017.04.046

Raji Y., Nadi A., Mechnou I., Saadouni M., Cherkaoui O. and Zyade S. (2023) High adsorption capacities of crystal violet dye by low-cost activated carbon prepared from Moroccan Moringa oleifera wastes: Characterization, adsorption and mechanism study. Diamond and Related Materials 135: 109834. https://doi.org/10.1016/j.diamond.2023.109834

Radaei E., Alavi Moghaddam M.R. and Arami M. (2014) Removal of reactive blue 19 from aqueous solution by pomegranate residual-based activated carbon: optimization by response surface methodology. Journal of Environmental Health Science and Engineering 12: 1-8. https://doi.org/10.1186/2052-336X-12-65

Ramutshatsha-Makhwedzha D., Mavhungu A., Moropeng M.L. and Mbaya R. (2022) Activated carbon derived from waste orange and lemon peels for the adsorption of methyl orange and methylene blue dyes from wastewater. Heliyon 8: e09930. https://doi.org/10.1016/j.heliyon.2022.e09930

Sujiono E., Zabrian D., Zharvan V. and Humairah N. (2022) Fabrication and characterization of coconut shell activated carbon using variation chemical activation for wastewater treatment application. Results in Chemistry 4: 100291. https://doi.org/10.1016/j.rechem.2022.100291

Tripathy A., Mohanty S., Nayak S.K. and Ramadoss A. (2021) Renewable banana-peel-derived activated carbon as an inexpensive and efficient electrode material showing fascinating supercapacitive performance. Journal of Environmental Chemical Engineering 9: 106398. https://doi.org/10.1016/j.jece.2021.106398

Williams N.E., Oba O.A. and Pasaoglulari Aydinlik N. (2022) Modification, Production, and Methods of KOH-Activated Carbon. ChemBioEng Reviews 9: 164-189. https://doi.org/10.1002/cben.202100030

Xing X., Zhang Y., Zhou G., Zhang Y., Yue J., Wang X., Yang Z., Chen J., Wang Q. and Zhang J. (2023) Mechanisms of polystyrene nanoplastics adsorption onto activated carbon modified by ZnCl2. Science of The Total Environment 876: 162763. https://doi.org/10.1016/j.scitotenv.2023.162763

Yorgun S. and Yıldız D. (2015) Preparation and characterization of activated carbons from Paulownia wood by chemical activation with H_3PO_4. Journal of the Taiwan Institute of Chemical Engineers 53: 122-131. https://doi.org/10.1016/j.jtice.2015.02.032

Zhang G., Yang H., Jiang M. and Zhang Q. (2022) Preparation and characterization of activated carbon derived from deashing coal slime with $ZnCl_2$ activation. Colloids and Surfaces A: Physicochemical and Engineering Aspects 641: 128124. https://doi.org/10.1016/j.colsurfa.2021.128124

Zhou J., Luo A. and Zhao Y. (2018) Preparation and characterisation of activated carbon from waste tea by physical activation using steam. Journal of the Air and Waste Management Association 68: 1269-1277. https://doi.org/10.1080/10962247.2018.1460282

Zhu G.-z., Deng X.-l., Hou M., Sun K., Zhang Y.-p., Li P. and Liang F.-m. (2016) Comparative study on characterization and adsorption properties of activated carbons by phosphoric acid activation from corncob and its acid and alkaline hydrolysis residues. Fuel Processing Technology 144: 255-261. https://doi.org/10.1016/j.fuproc.2016.01.007

Zięzio M., Charmas B., Jedynak K., Hawryluk M. and Kucio K. (2020) Preparation and characterization of activated carbons obtained from the waste materials impregnated with phosphoric acid (V). Applied Nanoscience 10: 4703-4716. https://doi.org/10.1007/s13204-020-01419-6

Zubir M.H.M. and Zaini, M.A.A. (2020) Twigs-derived activated carbons via H3PO4/ZnCl2 composite activation for methylene blue and congo red dyes removal. Scientific Reports 10: 14050. https://doi.org/10.1038/s41598-020-71034-6